

# Orthogonal Megatrend Intersections: “Coils” of a Stellar Transformer (Extended) Investigating the Southeast Indian Ridge Circuit

1<sup>st</sup> Published In: *Proceeding 11<sup>th</sup> International Multi-Conference on Complexity, Informatics, and Cybernetics*,  
pp. 61-66, Orlando, FL, March 2020

**N. Christian Smoot - Sr. Fellow (christiansmoot532@gmail.com)**  
**Geoplasma Research Institute (GRI)**  
**Hoschton, Georgia 30548 USA**

**Bruce Leybourne - Research Director**  
**Geoplasma Research Institute (GRI)**  
**Aurora, Colorado 80014 USA**

## ABSTRACT

According to the plate tectonic hypothesis, Fracture Zones (FZs) are considered transform faults that lie perpendicular to mid-ocean ridge axes; that is, they show the direction of seafloor spreading. Bathymetric maps of the Pacific Ocean basin exhibit a multitude of latitudinally trending FZs as well as longitudinally trending FZs on the Pacific plate. Analysis reveals that oceanic rises and plateaus generally sit atop the intersections associated with these leaky magmatic FZ intersections, exhibiting continental blocks, large igneous outpourings, and/or tectonic vortex structures at the intersections. Linear seamount chains correspond directly with many of these FZs. Thus, by the early 1980s many FZs were found to be active features with magma leakage along trend, shifting the concept that linear seamount chains must form as hot spot traces. With these clues and near total multi-beam bathymetry coverage in some ocean basins along with 1st order Geodetic Earth Orbiting Satellite (GEOSAT) structural trends the concept of intersecting megatrends evolved. How can the plate be spreading in several directions at the same time? Additionally, these megatrends are shown to continue into the continents, such as the Murray and Mendocino FZs in the northeastern Pacific, intersecting and crossing, the San Andreas Fault trend in California. The intersecting megatrends exhibit magnetic anomaly patterns related to magmatic intrusive/extrusive events not necessarily corresponding to seafloor foundation of Archean (original lithosphere) crust 4 – 2.5 billion years ago. Evidence of orthogonally intersecting megatrends coupled with a dubious interpretation of seafloor magnetic lineation age hypothesis leads investigators toward a more robust explanation of tectonic events. By understanding plasma tectonics is driven by space weather, where orthogonal FZs act as “coils” of a Stellar Transformer. The intersecting megatrends exhibit magnetic anomaly patterns reflecting ages of magmatic extrusion events into original Archean crust within the continents and ocean basins. In the ocean basins much of this Archean crust appears to have been “stripped off” from repeated Interplanetary Lightning strikes (static electricity), or Arc Blasts. A new paradigm emerges linking solar induction and space weather drivers of seismic and volcanic energies, the timing and global distribution of lightning data demonstrates a Solar Induction affect along these megatrends considered as “Coils” of the Stellar Transformer.

**Keywords:** Fracture Zones, Megatrends, GEOSAT, Orthogonal Intersections, Bathymetry, Stellar Transformer, Solar Induction, Plasma Tectonics, Mantle Circuits, Tectonic Vortex, Interplanetary Lightning, Arc Blast

## 1. INTRODUCTION - STATEMENT OF FACTS

By 1966 pundits had presented us with the plate tectonic hypothesis based on sketchy magnetic lineaments in the Gulf of Alaska coupled with a rudimentary outline of several fracture zones (FZs) in the North Pacific Ocean basin. The FZs were predicted to show the direction of seafloor spreading as they moved away from the influence of the ridge-crossing transform faults. This meant that they were locked and strong; in other words, dead. This was immediately called to question as the proposed FZs in the Pacific Basin (Fig.1 and 2) all converged in a fan-shaped pattern on the west of that basin [1].

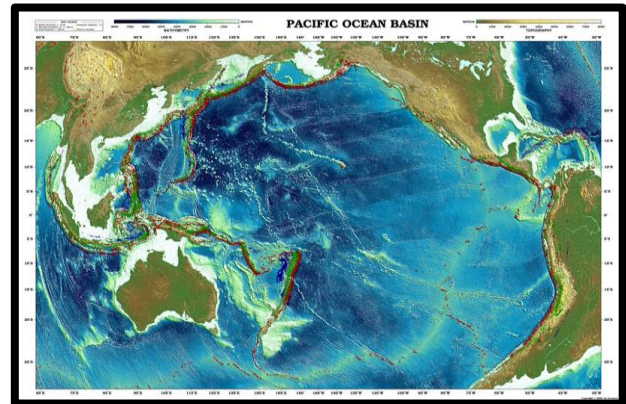


**Fig.1.** The National Geophysical Data Center (NGDC) produced a 1 arc-minute model of Earth’s surface, which includes topography and bathymetry in 2008. Called **ETOPO1** the Pacific Ocean basin orthogonal megatrend patterns become immediately apparent.

Obviously, for the hypothesis to fit FZs must be parallel on the same plate as the seafloor could not be spreading in more than one direction at any given time for that particular plate by definition. Of interest here, too, is the huge region in the western Pacific of the Jurassic and Cretaceous Magnetic Quiet Zones in which no anomalies were found at this early date [2]. Neither had any reliable rock ages been found from the scarce material that had already been sampled (any DSDP or ODP volumes). Additionally, no spreading ridge occurred between the northern end of the East Pacific Rise and the Juan de Fuca Ridge. This region was home to the major FZs such as the Chinook, Surveyor, Mendocino, Pioneer, Murray, Molokai, Clarion, Clipperton, and Galapagos FZs, all trending ENE-WSW, stopping at the mythical Darwin Rise, and all north of the equator [3, 4, 5]. Those in the southern hemisphere include

the Easter, Chile, Eltanin, and Udintsev FZs, the paucity of which may be a factor of little or no bathymetry. They generally trend ESE-WNW.

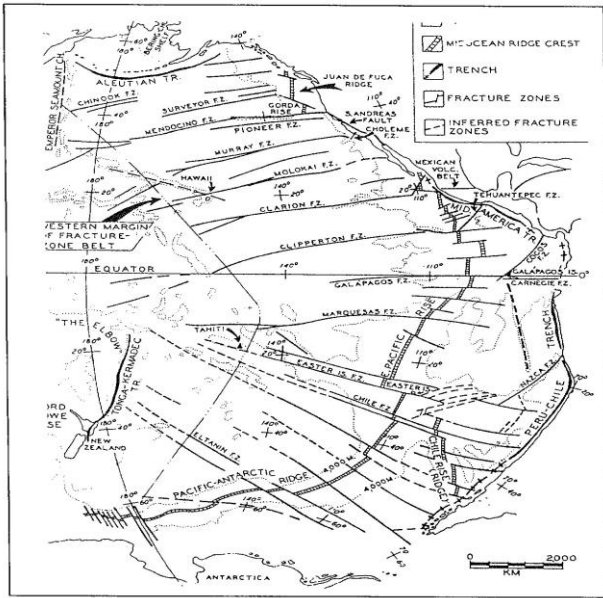


**Fig. 2.** 1972 interpretation of the fracture pattern for the Pacific Ocean basin. The Meyerhoffs, father and son [1], were completely ignored when they questioned the utility of explaining the direction of seafloor spreading. They realized that the Pacific “plate” could not be spreading in multiple directions.

## 2. MEGATREND CONSTRUCTION HISTORY

Ocean floor mapping of the northern Gulf of Alaska by the USS PIONEER and multi-beam sonar mapping of the northern and western Pacific basin by the USNS MICHELSON and the USNS DUTTON in the 1970s introduced the NNW-SSE trending FZs into the data base of the already well-known San Andreas and Queen Charlotte transform faults on the same axis (Fig. 3). Those included the Kashima FZ (originally named Heffner’s Fault; [6], the Mamua, Krusenstern, Stalemate/Emperor [7], Rat Island, Amlia, and Adak FZs. Non-parallel hotspot trails of linear seamount chains had also been delineated, such as the Emperor Seamounts, Hawaiian Islands, Ratak and Ralik parallel seamount/island chains, The Louisville Ridge, Line Islands, Liliuokalani Ridge, Tuamotu and Tubuai chains, etc. All were explained as the difference between relative and absolute plate motion over the proposed hotspots with a change in direction at 43 Ma.

Surveys in 1982/83 found seamounts/volcanoes being formed along the Murray and Mendocino FZs, thus belying the idea of locked and strong features [8]. Several exercises, such as using the guyot heights across the NW basin and combining the linear seamount chains lying in a direct line with the FZs, eventually produced the idea that the E-W FZs crossed the entire basin and intersected the N-S trending FZs in Fig. 3, [9, 10, 11, 12, 13, 14]. This combination of in-line features was named “megatrends”.

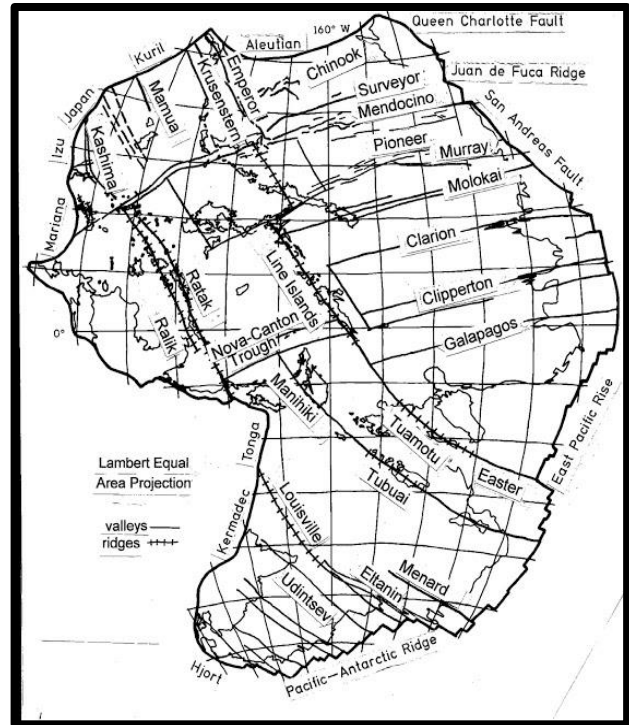


**Fig. 3.** 1988 Pacific Megatrend Pattern utilizing multi-beam and single-beam sonar data, even though southern ocean data coverage were sparse to non-existent. The 43 Ma bend in the Hawaiian Emperor seamount chains were extensions and parts of fracture zones indicating basin-wide lineaments now intersected others [15].

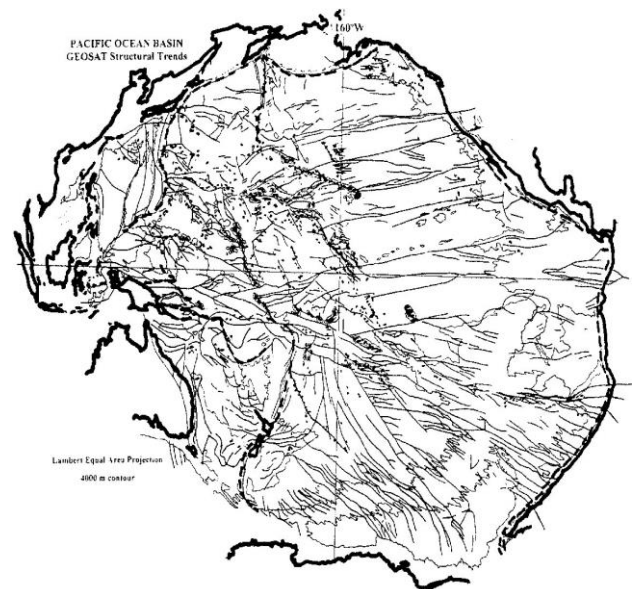


**Fig. 4.** 1995 High-Pass Filtered GEOSAT Structure diagram of Pacific Basin. Most of the trends directionally splay from the trenches on the west to North and South American continents to the east, splaying at the distal ends. The morass of the seamount clusters in the NW basin is now brought more clearly into focus. Other ocean basins appear to be different ages than the Pacific basin, which has been declared to be at least 650 Ma. Fracture patterns in the Antarctic, Indian, and Atlantic basins also appear different implying the “coils” of the Stellar Transformer may have had different orientations in the past [16].

Constructing updated structural diagrams of the basin progressed from the use of the Digital Bathymetric Data Base 5-minute grid through the high-pass filtered Geodetic Earth Orbiting Satellite (GEOSAT) data (Fig. 4) and onto enough multi-beam data to update the General Bathymetric Chart of the Oceans (GEBCO) charts allowed for a re-interpretation of tectonic events for the Pacific basin [17, 18, 19]. This has since been updated to the ETOPO-1 database (Fig. 1). With very little accurate bathymetry in the southern Pacific basin, the structural trends, which have been verified by comparing those in the North Atlantic to the total coverage bathymetry, are valuable tools in making any kind of determination in relation to the regional tectonics. Be aware that, highly heated, or very active ridge systems such as the East Pacific Rise, features are not well delineated in the GEOSAT data set, since a lower density reduces the gravity signal (Fig. 4).

### 3. ORTHOGONAL MEGATREND INTERSECTIONS

The Murray and Molokai FZs come off their intersections with the San Andreas Fault and pass through the Musician's Seamounts and the eastern Hawaiian Ridge to intersect with the downward trend of the Mamua and another FZ to the west of that [20]. This influences the formation of the Mid-Pacific Mountains (Fig.5). To the west of that, following the Kashima FZ south through the Mapmaker seamount province and the Marcus-Wake seamounts/guyots leads to the intersection with the Mendocino FZ where the Ralik and Ratak (Marshall-Gilbert) seamount chains begin. This is central portion of the middle of the mythical Darwin Rise [4, 5, 12] where the regional base depth is about 5500m. The megatrend continues into a large province at the juncture as the Mid-Pacific trend crossing the Clarion FZ at the Magellan Plateau and intersecting the Clipperton and Galapagos FZs at the Manihiki Plateau.

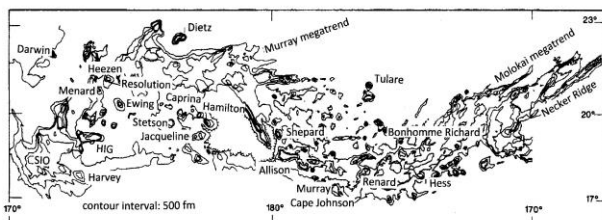


**Fig. 5. Bathymetry (top) and Tectonic Diagram (bottom)** of trends in the Mid-Pacific Mountains. Specifically, notice that the passage of the M-T megatrend from the NNW has heavily influenced the overall tectonic configuration of the center of the feature [11].

Features (Fig. 6) in the north-central Pacific Basin (30°-55°N; 155°E-175°W) expand on the aberrations [21]. Beginning at the Kuril and Aleutian trenches, the Obruchev Rise lies on a general NW-SE azimuth. It joins with the Emperor Trough (ET) megatrend after being overprinted by the Emperor Seamounts. Sub-parallel megatrends flank the ET, such as the Mamua, Krusenstern, and Stalermate FZs.

Standing by with that thought, the WSW-trending Chinook Trough is actually part of a megatrend by that name. Coming from its intersection with the Queen Charlotte Fault in Alaska, it intersects the SSE trending Emperor FZ into the region of the Hess Rise (HR; Fig. 6), and is possibly one of the leading features building the Shatskiy Rise (SR) as it continues to the Mariana Trench.

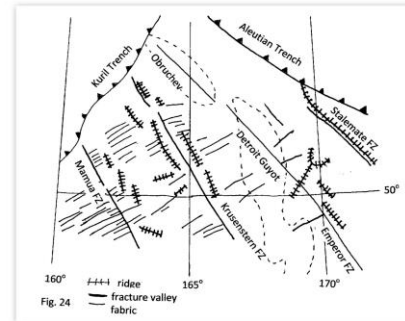
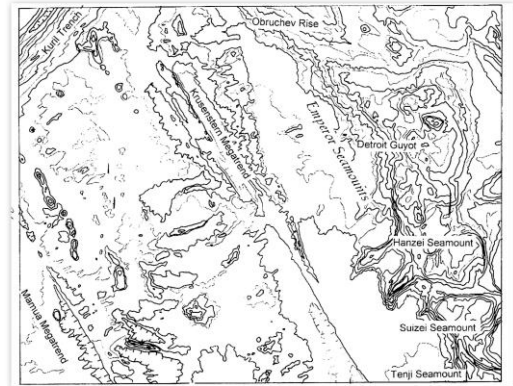


**Fig. 6. Bathymetry (top) and Structural Diagram (bottom)** of the north-central Pacific basin showing the abundant southeasterly-trending FZs that are associated with megatrends. Of primary interest here is the Obruchev Rise, which joins with the Emperor FZ [20].

South of the HR (Fig. 7, 8, and 9) the Surveyor and Mendocino megatrends merge at the southern end of the Emperor FZ. The southerly passing of the Emperor-Easter megatrend is offset and continues at the Liliuokalani Ridge, which passes through the Hawaiian chain, is offset to the west with the intersection of the Pioneer-Murray megatrend. There it becomes the Line Islands (Fig. 2). That trend continues to the SE where it intersects the Clipperton and Galapagos megatrends, passing through the Tuamotu Islands and the Easter FZ to the East Pacific Rise. With the Emperor Seamounts possibly being formed between 43 Ma and 73 Ma, and the Shatskiy Rise being formed about 140 Ma, and the HR being formed by whatever means at about 120 Ma, none of the ages and tectonic scenarios fit. The most practical solution is to have a region saturated with intersecting megatrends underlain by leaky heated channels with zero plate motion.

A similar exercise is possible with the Udintsev in toto, the Kashima-Ratak/Ralik-Louisville-Eltanin, and the Mamua-Manihiki-Tubuai-Chile megatrends. As of this writing, this exercise in the Indian, Southern, or Atlantic Ocean basins appear to have a different framework, because intersecting fracture/megatrends appear much different in the current bathymetry or the GEOSAT data.

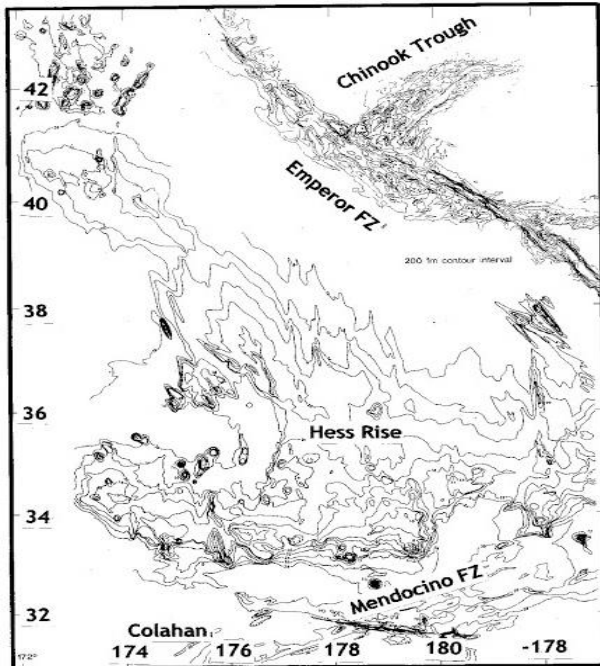


**Fig. 7. The Primary N-S Axis is Built by Fracture Leakage** of the fracture swarm megatrend coming out of the Kamchatka Peninsula. From the HR to the SR the Chinook megatrend is overprinted in the bathymetry. It does not appear in the GEOSAT data either, so it was probably the first in the region, and the HR was possibly built at a later time. Smaller sets of trends, such as the four small ridges on the north of HR [22], influence trends in the Emperor Seamounts and SR.

Many of the rises/plateaus seem to be primarily seamount clusters, such as the Dutton Ridge. Most of these have been determined to form in leaky fractures by magma leakage through zones of weakness in the overlying crust. This is particularly true at the intersections. Nelson Guyot in the NW Pacific basin sits atop the intersection of the Kashima [6] and Chinook megatrends. As the Chinook continues westerly, it intersects the southeasterly-trending Udintsev megatrend at the Ogasawara Plateau. As the Udintsev continues southerly, it intersects the Mendocino megatrend in the Dutton Ridge where the gross morphology reflects that crossing, possibly breaking up that plateau into the ridge [15, 19]. It may be the agent responsible for producing the western portion of the Ontong-Java Plateau before its passage is engulfed by the eastward migration of the trench system.

In keeping with the theme of this treatise, we question the origin of the rises and plateaus in relation to the intersections. Did they extrude through large weaknesses in Earth's crust? Does a layer of granite underlie the oceanic basalt layer? Has the original crust, whatever it may have been, been transformed by external forces, such as lightning from interplanetary discharges? Some of these intersections may be related to the plasma tectonic explanation as being coils of a stellar transformer. We also question why, with the San Andreas and Queen Charlotte Faults having already been known by 1966, why the intersections were not called to question in the formulation of the plate tectonic hypothesis. WHY?

The Murray and Molokai FZs (Fig. 2 & 3) pass through the Musician's Seamounts and the eastern Hawaiian Ridge to intersect with the downward trend of the Mamua and another

FZ to the west of that [20] and influence the formation of the Mid-Pacific Mountains. To the west of that, following the Kashima FZ south through the Mapmaker seamount province and the Marcus-Wake seamounts/guyots leads to the intersection with the Mendocino FZ where the Ralik and Ratak (Marshall-Gilbert) seamount chains begin. This is central portion of the middle of the mythical Darwin Rise [12, 4, 5] where the regional base depth is about 5500m. The megatrend continues into a large province at the juncture at the Mid-Pacific, crosses the Clarion at the Magellan Plateau, and intersects the Clipperton and Galapagos at the Manihiki Plateau.

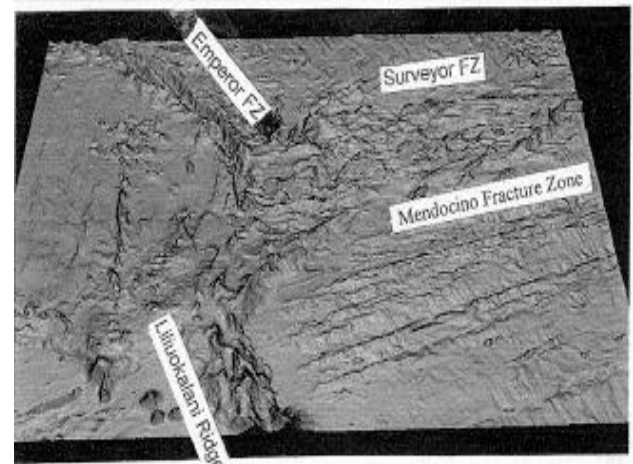


**Fig. 8. The Southern Boundary of HR is clarified** by using a 3D program, which employed anti-aliasing filters, a minimum curvature spline algorithm to generate a regional field, and a merge algorithm to blend input and region data to produce the final output grid. This was made possible by the original surveys with the 1°-beam width sonar package on a close order line spacing that ensured total bottom coverage. Now no confusion exists as to the geomorphology of intersection tectonics [20].

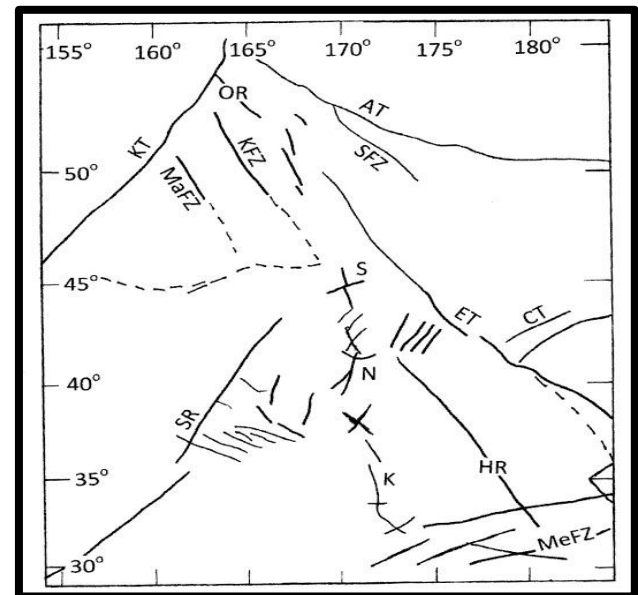


**Fig. 9. By combining the original Fig.2 with the updated data** from Fig. 3 and the total-coverage multi-beam sonar survey data this 2012 breakout map of the northwest Pacific demonstrates the fallacies of the plate tectonic hypothesis while reinforcing the intersecting megatrend idea [21].

Smaller sets of trends, such as the four small ridges on the north of HR [22], influence trends in the Emperor Seamounts and SR. The dashed line on the 45°N latitude line is from the GEOSAT diagram, and it is a trough. Last, the smaller chains of seamounts in the central SR lie on yet another azimuth.

With the Emperor Seamounts possibly being formed between 43 Ma and 73 Ma, and the Shatskiy Rise being formed at a triple junction about 140 Ma, and the Hess Rise being formed by whatever means at about 120 Ma, none of the ages and tectonic scenarios fit. The most practical solution is to have a region saturated with intersecting megatrends underlain by heated channels.

Plateaus and rises mostly occur at the orthogonal intersections, features such as the Ontong-Java, Ogasawara, Kerguelan, and Manihiki plateaus and the Hess, Shatskiy, Rockall, and Obruchev rises. These features have all been sampled profusely by the DSDP and ODP investigators along with many grab samples. Many of these features appear to be something other than basaltic in nature; that is, they are granitic. Some have been called sundered continental fragments.

#### 4. SOUTHEAST INDIAN RIDGE CIRCUIT

The fracture alignments in the Indian basin (Fig. 10) are confused by the inclusion of the three different Indian ridges and the composition of a huge vortex structure, the Rodrigues Triple Junction just west of Madagascar.

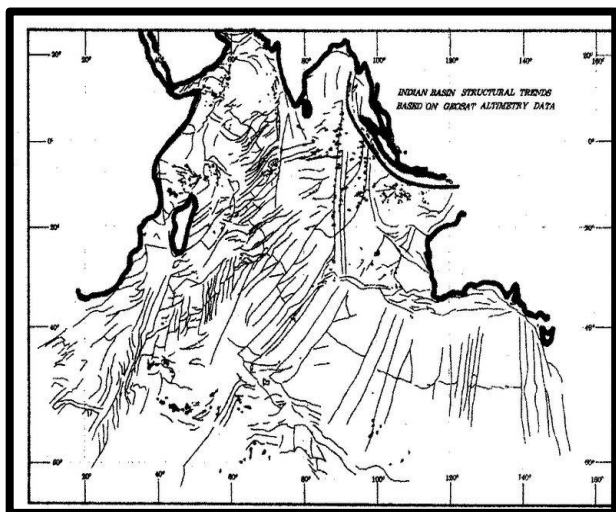


**Fig. 10. 1995 High-Pass Filtered GEOSAT Structural Diagram of the Indian Ocean basin [16].** The Rodrigues triple junction lies in the center. Primary alignments here are the Central Indian Ridge with the 90-east ridge and the Chagos-Laccadive Ridge. The large orthogonal intersection on the Antarctic region is home to the Kerguelan Plateau.

These first order megatrends have been established in the Indian Ocean Basin [15, 16, 19, 20] from bathymetric charts and Geodetic Earth Orbiting Satellite (GEOSAT) structural diagrams (Fig. 10). GEOSAT structural trends in the Indian Ocean Basin display orthogonal intersections where west meets east, at the Rodrigues Triple Junction (RTJ), along trends of the Southwest Indian Ridge (SWIR), Southeast Indian Ridge (SEIR) and Central Indian Ridge (CIR) intersection (Fig. 10, 11 & 12).

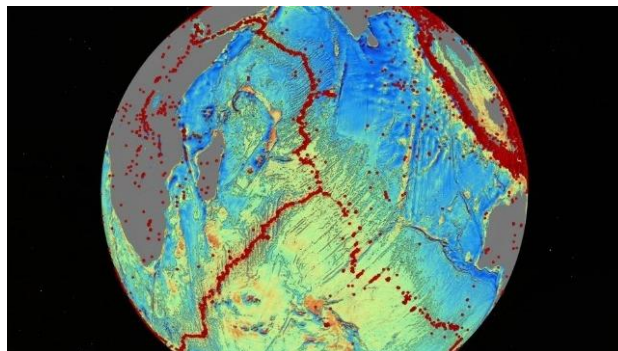


**Fig. 11. Sea Floor Map** reveals details about earthquakes (red dots), sea floor-spreading ridges and faults along the Rodrigues Triple Junction. (David Sandwell -UCSD) [https://www.navy.mil/view\\_image.asp?id=9045&t=4](https://www.navy.mil/view_image.asp?id=9045&t=4)

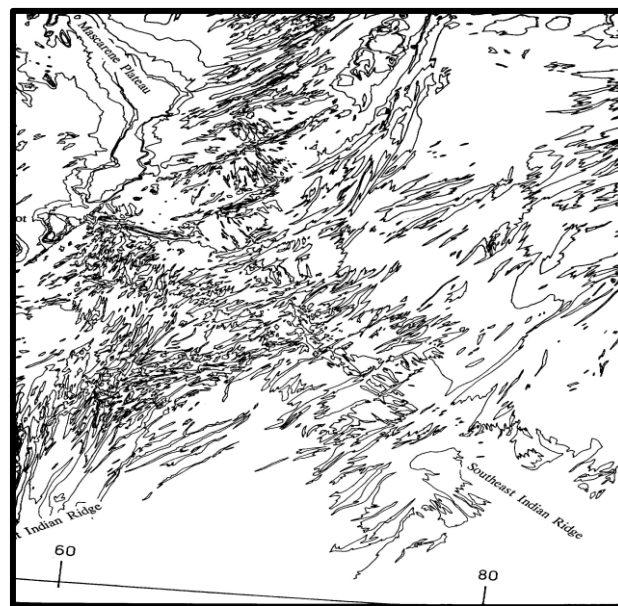


**Fig. 12. High Resolution Bathymetry of the Rodrigues Triple Junction (RTJ) near 28°S & 70°E in the southern Indian Ocean Basin** compiled by Smoot using ship-of-opportunity data overlain with GEOSAT data, which was used to guide the fracture zone orientation.

These Indian Ocean Basin fracture alignments are confused by the inclusion of the three different ridges superimposed by this huge Tectonic Vortex [1] (Fig. 13) structure or Triple Junction. Triple Junctions, thus Tectonic Vortexes, are fairly common worldwide: such as the Rivera; Galapagos; Banda Sea; Easter Island/Juan Fernandez; and Macquarie in the Pacific; the Bouvet in the Atlantic; and the Rodrigues and Afar in the Indian ocean Basins. Higher resolution (Fig. 12) maps the Rodrigues Triple Junction (RTJ) near 28°S & 70°E in the southern Indian Ocean Basin. Since it was originally mapped, many different explanations have been presented as to its formation and wanderings [23, 24, 25, 26].

Studies involving the use of magnetics show spreading on the CIR/SEIR axis to be NE and SW on either side of the mid-ocean ridge(s). For the SWIR those directions are NNW and SSE [23, 24]. The RTJ has been subjected to sporadic ridge jumps, while the path has been continuous for the past 75 Ma as a Ridge-Ridge-Ridge (R-R-R) feature [24]. The CIR, with its relatively fast 6 cm/yr. spreading rate, and the SEIR with its 5

cm/yr. spreading rate join the super slow-moving SWIR with its 1.6 cm/yr. spreading rate [27]. Based on gravity calculations, the SWIR shows no indication of lithospheric growth [28]. Tomography of the mid-ocean ridge studies show the SWIR to be deep-rooted at 250-300 km [29]. The same studies of the CIR and SEIR show that those are shallow rooted at about 100 km. As all these ridges approach within 900-1000 km of the RTJ, strong low seismic velocities zones that extend down to 100 km characterize them. However, the SWIR with its 4300 and 5000-m-deep valleys cannot close at the RTJ because it is also claimed to be a Ridge-Ridge-Fracture (R-R-F) mode. Therefore, it is unstable [30].

## 5. MODELING THE RODRIGUES TECTONIC VORTEX

The Rodrigues Vortex preferentially moves eastward [1] and is a large counterclockwise rotating vortex along the SWIR controlling triple junction dynamics (Fig. 13). In the southern hemisphere, this generally means a high-pressure down welling mantle vortex with westward asthenosphere counter flow [31]. Many of the rises/plateaus along these *Orthogonally Intersecting Megatrends* seem to be primarily seamount clusters. Most of these have been determined to form in leaky fractures by magma leakage through zones of weakness in the overlying crust. The Deep-Sea Drilling Program (DSDP), and Ocean Drilling Program (ODP) have sampled many of these features profusely; along with many grab sample investigations [5]. Many of these features appear to be something other than basaltic in nature; that is, they found granite in some places. Some have been called sundered continental fragments [5] or possibly they are remnants leftover from “Arc Blast” [32] stripping of crustal material?

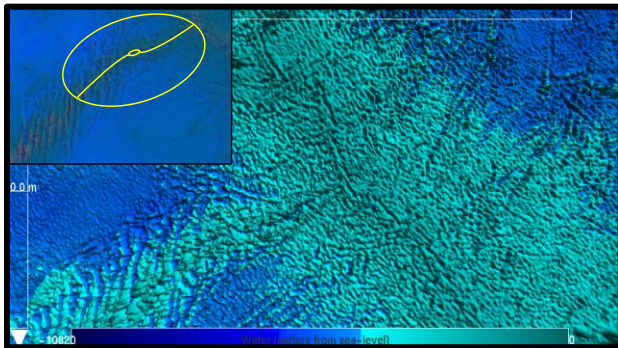


**Fig. 13. Tectonic Vortex** upper inset overlay over 2 min. Digital Bathymetry Data Base (DBDB-2') in Climate Scope Visualization of the Rodrigues Triple Junction (RTJ).

Viewing the RTJ from the southwest in 3-D bathymetry (Fig. 14) a series of smaller vortices in zoom view (Fig. 15) is delineated. In plate tectonic terms these are called Overlapping Spreading Centers (OSC). Figure 5 clearly shows a double comma vortex signature in almost every case along these fracture offsets. The vortex signature is counter clockwise for these smaller vortices indicating upwelling (low pressure) in the asthenosphere counterflow.

Most mid-ocean ridge fracture systems exhibit these type vortex signatures, thus there is evidence for an underlying upper mantle flow structure with a counter flow in the asthenosphere, i.e. within the magmatic system along the ridge strike. These features are globally ubiquitous and indicate underlying flow structures.

In keeping with the theme of this treatise, we question the origin of the rises and plateaus in relation to the intersections. Did they extrude through large weaknesses in Earth's crust? Does a layer of granite underlie the oceanic basalt layer? Has the original crust, whatever it may have been, been transformed by external forces, such as lightening from interplanetary discharges? Can granite be electrically transmuted from magmatic elements?

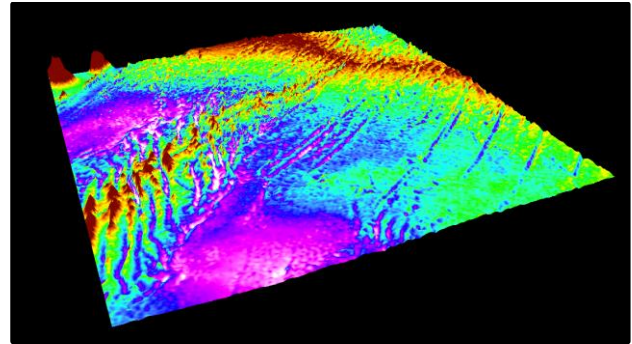


**Fig. 14. 3-D Bathymetry** shows the Rodrigues Triple Junction (RTJ). NOAA – ETOPI [33].

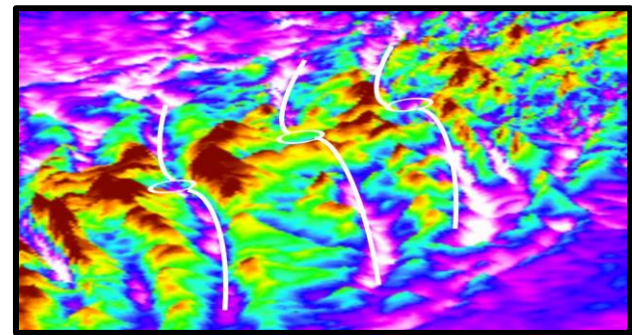


**Fig. 15. 3-D Bathymetry** portrays overlapping spreading center (a series of smaller vortices), along the SWIR leading toward the Rodrigues Triple Junction (RTJ) in Fig. 14 NOAA – ETOPI [33].

## 6. RIDGE INDUCTION AFFECTS LIGHTNING TELLS THE STORY [34]

National Aeronautics and Space Administration (NASA) launched Optical Transient Detector (OTD) in 1995 to 2000, a prototype of the Lightning Imaging Sensor (LIS) instrument launched in 1997 to 2015. These were specifically designed to detect *Lightning* from space during both day and night with storm-scale resolution. Earth's *Lightning* hotspots were revealed with very high-resolution *Lightning* climatology derived from 16 years of space-based Lightning Imaging Sensor observations. Analysis and results published in 2016 [34] revealed, “Where are the lightning hotspots on Earth?” For years, African Congo (right - Fig. 16) was known as the *Lightning* Capital of the World, while the Tampa Bay, Florida area was unofficially known as the “*Lightning* Capital of the United States.” Also sometimes called “*Lightning* Alley”, but in 2016 with the new *Lightning* analysis [34], the *Lightning* hotspot location moved about 30 miles southeast of Fort Myers Florida, while Catatumbo *Lightning* (upper left – Fig. 16), became the new *Lightning* Capital of the World at Lake Maracaibo, on the coast of Venezuela. Or possibly the new data may have clarified that the hotspot location was originally in these locations, without prior years data to 1995 this is an unknown.

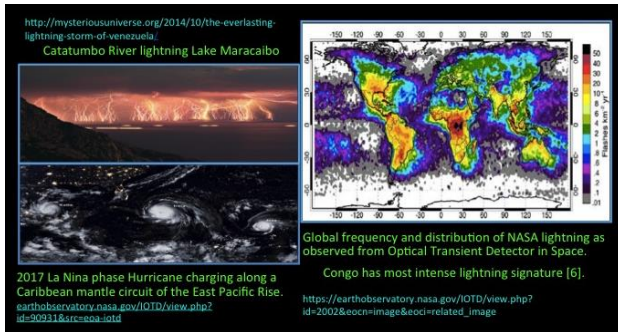


**Fig. 16. Catatumbo Lightning** (upper left image), and Intense African Congo *Lightning* from NASA (upper right image). Irma, Katia, Jose (lower left image) charging the Earth along a Caribbean mantle circuit. The African Congo *Lightning* flash global frequency and distribution of *Lightning* as observed from space by the Optical Transient Detector (upper right image) shows Congo with most intense *Lightning* signature [35].

What made the global *Lightning* distribution shift from Africa to South America? And why was there a corresponding shift in Florida from Tampa Bay to Ft. Meyers? There seems to be a simple *Electro-Magnetic* attraction from *Solar Induction* affects the inline vortex (with spin of the earth) ridges structures of our planet associated with the East Pacific Rise and northern component of the Southeast Indian Ridge “hot circuits”. Induction heating along the “HOT” ridges indicated by change in global distributions of *Lightning*, alternatively heats the Southeast Indian Ridge (SEIR) from Radial Induction, and then shifts to the East Pacific Rise during Axial Induction (Fig. 17). Return circuits along the Western Pacific Rim and Mid-Atlantic Ridge at times may also become active. These upper *Mantle Circuits* connect with inner/outer core circuits at the poles [36].

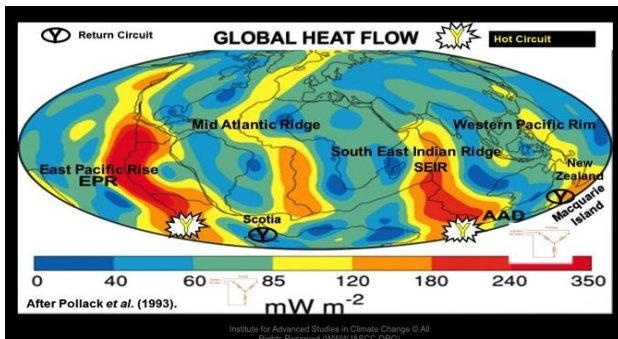


**Fig. 17. Global Heat Flow** from induction heats ridges alternatively heating the Southeast Indian Ridge (SEIR) during axial induction, and then shifts to the East Pacific Rise during radial induction. Most induction affects would be more complex than this simple explanation. Modified after Pollack et al. (1993).

### Congo and the South East Indian Ridge (SEIR)

Earth’s second greatest *Lightning* hotspot is in the Congo near the border of Rwanda on the west side of the Mitumba Mountains (Fig. 18). The Mitumba Mountains at the eastern edge of the Congo basin mark the beginning of the Western Rift Valley in East Africa. Greater *Lightning* flash rate densities are observed along a continuous large area on the western foothills of these mountains from 4°S to 5°N, having 6 out of the 10 African hotspots. Ba and Nicholson in 1998 [37] found that maximum convection occurs during the morning (0500–0800 LST). Interestingly this is the period the Mid-Atlantic Ridge

goes through midnight; about the same time the Western Pacific Rim aligns with noon and the South Pole offset toward Australia indicating the possibility of a ridge induction affect [38].

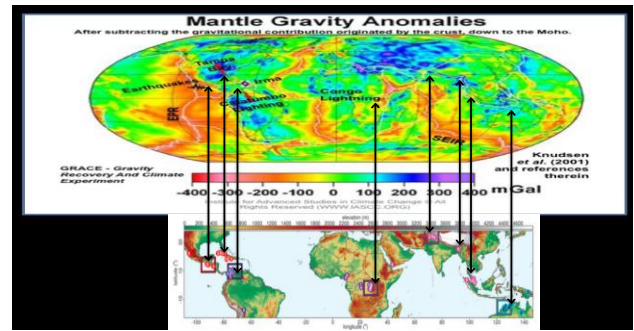


**Fig. 18. Lightning Hotspots** (lower insert [34]), Relationships to Mantle Gravity Circuits (upper insert [39]). Although coastal relationships to *Lightning* exist in many instances, most if not all *Lightning* hotspots appear related to mantle circuit termination points associated with rift, rivers and lake systems within continents as well as nearby planetary scale vortex structures adjacent to circuits.

*Lightning* hotspots over the Mitumba Mountains exhibit higher mean diurnal cycle flash rates during the afternoon from 1500 to 1700 LST than in the central Congo at 1500 LST, with some activity during the night. The 1500 afternoon local time 3 hour offset from noon suggests an induction affect from alignment of the north component of the SEIR associated with the Rodriguez Triple Junction, a tectonic vortex coincidentally 3 time zones to the East of the African continental rift. This north-south trend of the SEIR also directly aligns with the Pakistan *Lightning* area at the head of the Indus River. Large river fracture systems are tied to many of these lightning grounding zones. Thus, the main induction element to monitor for this general region is the northern component of the SEIR.

Lake Victoria (as well as other lakes along the East African Rift Valley) also exhibits deep nocturnal convective activity likely from a direct induction affect from African Rift alignment at midnight. Thunderstorms occur year-round in central and western Africa, but these regions are electrically more active from September to May during the northern hemisphere wintertime, when South Pole faces sun and SEIR has a larger induction affect. Less *Lightning* activity is observed in July when North Pole faces sun.

## 7. ATLANTIC BASIN

Figure 19 carries the GEOSAT structural trends into the Atlantic basin, neither of which display the absolute orthogonal intersections of the 750-million-year-old Pacific Basin. The Atlantic basin (Fig. 19) does show the braiding, anastomosing pattern of the megatrends however and their orthogonal intersections with the Mid-Atlantic Ridge. These “Coils” of a Stellar Transformer may have been organized much differently when these Ocean Basins were formed or have possibly been modified by some more recent event or cataclysm, yet to be understood or explored. The opposing orthogonal patterns in the North vs. South of the Atlantic Basin implies some difference in the “Coils” possibly confined to the northern vs. southern hemispheres long ago.

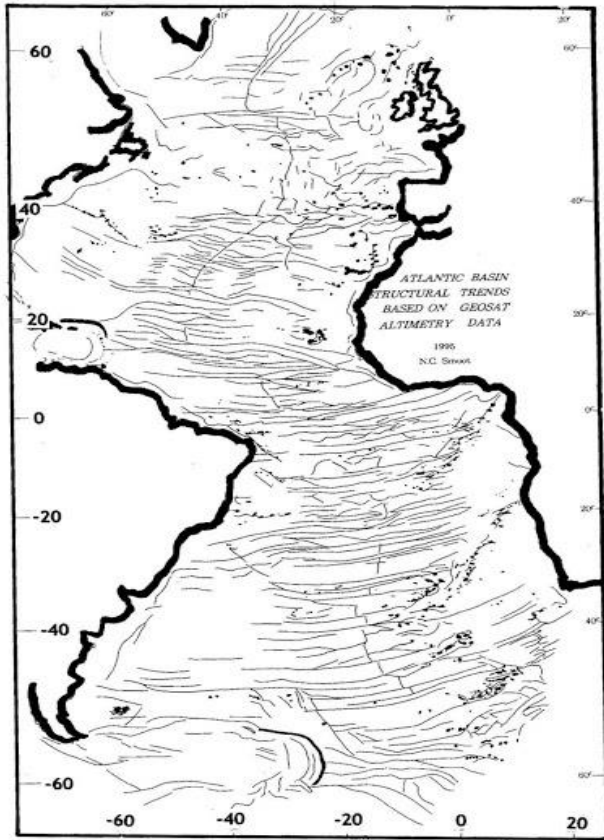


**Fig. 19. 1995 High Pass Filtered GEOSAT Structural Diagram** of the Atlantic Basin showing non-linear alignments of the fractures [16].

## 8. PLATE INTERPRETATIONS

Once spreading rifts entered the conversation ~1965, and then plates were defined ~1966 more-or-less, the scramble began to define the spreading directions and rates. By 1966 pundits had presented us with the plate tectonic hypothesis based on sketchy magnetic lineaments [40] in the Gulf of Alaska coupled with a rudimentary outline of several fracture zones (FZs) in the North Pacific Ocean basin. The FZs were predicted to show the direction of seafloor spreading as they moved away from the influence of the ridge-crossing transform faults. This was immediately called to question as the proposed FZs in the Pacific Basin all converged in a fan-shaped pattern on the west of that basin [1]. Later it was found that there were no reliable magnetic basement rock ages found in material sampled by the Deep-Sea Drilling Project (DSDP) or the Ocean Drilling Program (ODP) [5]. Theoretically for plates to fit FZs must be parallel on the same plate, as the seafloor could not be spreading in more than one direction at any given time for that plate by definition. Nor can the plate be spreading in several directions at the same time.

By 1974 a worldwide effort produced an updated bathymetric database of the world's ocean basins [5]. Robert Fisher of Scripps compiled the original map of the Indian Ocean showing a triple junction comprised of the Southwest Indian Ridge (SWIR), the Southeast Indian Ridge (SEIR), and the Central Indian Ridge (CIR). Having several descriptors, the RTJ has been described as moving, remaining stationary, to be made up

of ridge-ridge, ridge-ridge-transform, and many different configurations of each, although, the CIR and the SEIR appear to lie on essentially the same azimuth [25].

## 9. "COILS" OF A STELLAR TRANSFORMER [38]

Understanding our planets *Endogenous Energy* [41] and its link to solar drivers with the *Stellar Transformer* [38] concept can be considered as part of the scientific abstraction process that is at the basis of the exploratory analysis, as emphasized by John Tukey in 1977 [42]. This is preliminary to complete science, i.e. before the confirmatory analysis that must be carried out to check the inferred consequences by means of observations.

In space above the earth's poles there are aurora plasma rings, inducing ground currents within the mid-ocean ridges, especially the mid-ocean ridge encircling the South Pole (*Radial Induction*) (Fig. 20). Mantle circuit trends can be mapped with satellite mantle *Gravity* imaging (Fig. 21) of the thermal signatures (Fig. 17) given off by induction current elements of the mid-ocean ridge circuits. Complex *Magnetic Modeling* techniques reveal multi-phase circuit configurations of the Polar Regions, reviewed in previous writings "*Evolution of Earth as a Stellar Transformer*" [36]. For example, circuit activation and switching of these global scale electric circuits can be understood in terms of shifting *Earthquake* and *Lightning* hotspot activity. The SEIR mantle circuit provides South Pole grounding links to lighting activity in the African Congo. A global momentum shift in *Lightning* from the African Congo to Lake Maracaibo, Venezuela occurs in conjunction with the 11-year sunspot cycle and signals a change of Earth's charging phase, which switches to the East Pacific Rise.

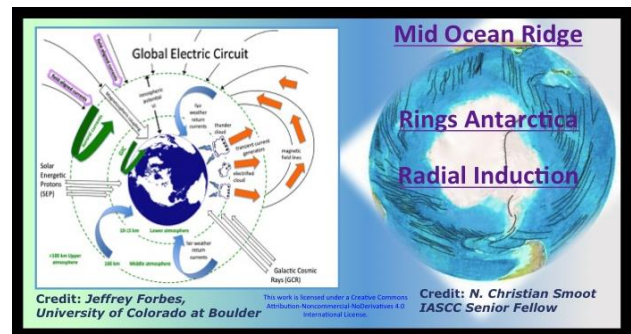


**Fig. 20. GLOBAL ELECTRIC CIRCUIT** Conventional Model includes Ground Inductions Currents (GIC) magnetically coupled to Aural Ring Currents torqued by Field Aligned Induction currents from magnetosphere coupling to solar forcing. (Forbes, J. - University of Colorado – Boulder). Step down aurora energy to the Mid-Ocean Ridges encircling Antarctica would generate powerful radial ground induction currents (Smoot, N.C. - Sr. Fellow IASCC).

Thus, by understanding tectonics as a plasma process driven by space weather, orthogonal FZs act as "coils" of a stellar transformer [43]. These intersecting megatrends also exhibit magnetic anomaly patterns reflecting ages of magmatic extrusion events into "stripped off" original Archean crust from repeated Interplanetary Lightning strikes (static electricity), or Arc Blasts [32, 44]. A new paradigm emerges linking solar induction and space weather as drivers of seismic and volcanic energies, magma production, climate, weather effects, and

sparkling electrical wildfire outbreaks at continental borderlands. The timing and global distribution of lightning data demonstrates a solar induction effect along these megatrends considered as Circuits of a Stellar Transformer.

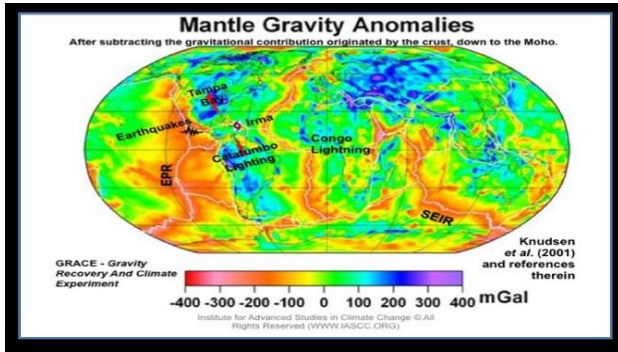


**Fig. 21. Mantle Gravity Anomalies** from GRACE satellite mission data [39] indicate East Pacific Rise (EPR) polar and continental circuit connections to Catatumbo, Tampa Bay Lightning anomalies, and Southeast Indian Rise (SEIR) connections to the African Rift/Congo global lighting anomalies.

*Electro-Magnetic or Magnetic* induction is the production of an electromotive force, or voltage, across an electrical conductor in a changing *Magnetic* field. The *Stellar Transformer Concept* [36, 38] (Fig. 22) contends that simple step down energy induction occurs between sun and earth, much like the transformer process that steps down your household energy from higher voltage transmission lines sourced from the power company.

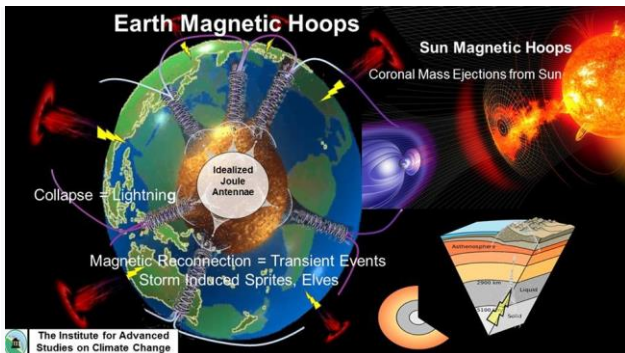


**Fig. 22. Earth as a Stellar Transformer** idealized *Plasma Core Planetary Electronics* based on Sea Urchin Spike Model [41] as anodes tufts (Safire Project 2017 <http://safireproject.com/>) See: *Electric Universe 2015* Presentation <https://www.iascc.org/free-stuff>.

The sun would represent a large coil from the power company, while the earth represents the smaller coil to your home. The larger coil element generally excites current into the smaller coil element by induction of “step down energy”. Layers within the Earth hold and release charge acting as condensers, or capacitance layers. Thus the larger Stellar Transformer hypothesis concludes that induction characteristics are determined by the Earth’s *Magnetic Moment*<sup>1</sup> representing the *Magnetic*

<sup>1</sup> The *Magnetic Moment* is defined as a quantity that represents the *Magnetic* strength and orientation of a magnet or other object that produces a *Magnetic* field. The *Magnetic Dipole Moment* of an object is defined in terms of the torque the object experiences in a given

*strength and orientation that produces Magnetic field current alignments between layers in the Earth and polarity and field strength* primarily considered in relationship to the Sun and Moon and to a lesser extent other planets related to the total Interplanetary Magnetic Field (IMF) within which the Earth resides. Vector induction components of torque generating power for Earth’s magnetic moment are outlined below.

Earth’s Vertical (z) induction effects, associated primarily with magnetic moment linked to Sun-moon tidal variations affecting volcanic and magmatic electric joule energy production of sea-urchin spines or anode plasma tufts. Considered connectors between the oppositely (+/-) charged double layers of the radial-toroidal (*E*) and axial-poloidal (*E*) electric fields. Using a model similar in nature to a “sea-urchin”, Gregori explains the propagation of electrical “Joule” energy along these “sea urchin” spines (Fig. 22 and 23) to Earth’s core and geologic hotspots around the globe [41].

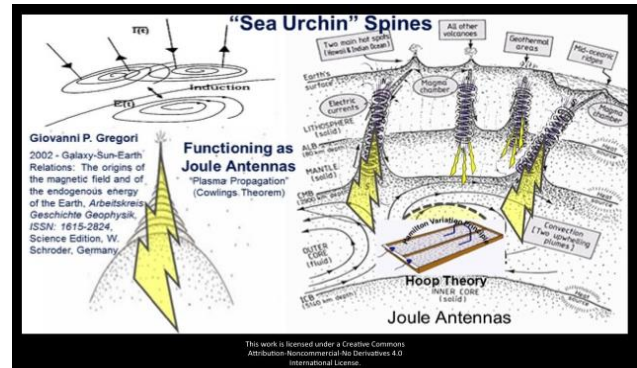


**Fig. 23. Earth “Internal” Sea Urchin Spike/Antenna** Adding to conventional Earth Model the concept of electrical potential joule spikes emanating from a plasma core. [41].

Earth’s Axial (y) dipole induction effects of the poloidal (*E*) electric field primarily on polar connected north-south circuits of the mid-ocean ridges, western Pacific rim, and inner core, associated with magnetic moment of the total field strength and polarity variability of mostly the sun, moon and planetary orientation can be large especially as related to position of Earth’s liquid outer core. A direct coupling with the Earth’s most powerful induction current elements occurs within its mantle and inner/outer core. Mantle circuit trends can be mapped with satellite mantle *Gravity* imaging of the thermal

*Magnetic* field. The strength and direction of this torque depends not only on the magnitude of the *Magnetic Moment* but also on its orientation relative to the direction of the *Magnetic* field and is therefore *considered a vector*. The direction of the *Magnetic Moment* points from the South to North Pole within the magnet in this case the Earth. The magnetic field of a *Magnetic Dipole* is proportional to its *Magnetic Dipole Moment*. The dipole component of an object’s magnetic field is symmetric about the direction of its *Magnetic Dipole Moment*, and decreases as the inverse cube of the distance from the object. The strength of a *Magnetic Dipole* is called the *Magnetic Dipole Moment*. *Considered a measure of a dipole’s ability to turn itself into alignment within a given external magnetic field*. In a uniform magnetic field, the magnitude of the dipole moment is proportional to the maximum amount of torque on the dipole, which occurs when the dipole is at right angles to the magnetic field. The *Magnetic Dipole Moment*, often simply called the *Magnetic Moment*, may be *defined then as the maximum amount of torque* caused by magnetic force on a dipole that arises per unit value of surrounding magnetic field in vacuum (Wikipedia & Britannica).

signatures given off by induction current elements of the mid-ocean ridge circuits (Fig. 21).

Earth's Radial (x) induction effects of the toroidal (E) electric field, associated primarily with variations of the magnetic moment of solar winds magnetic field strength and polarity variability primarily affecting Earth's outer core and E-W oriented "orthogonal" fracture systems are the "COILS" of the Earth component of a Stellar Transformer. IMF polarity determines which orthogonal system swithes on and the direction of energy flow through the planet, indicating earth is set in an *Alternating Current (AC)* space environment. The south pole has most energy transfer from a ring effect along the ridge encircling Antarctica (Fig. 20). In space above the earth's poles the aurora plasma rings, induce ground currents within the mid-ocean ridges, especially the mid-ocean ridge encircling the South Pole (*Radial Induction*), transformer "COILS" (Fig. 20).

Joule energy in this sense means "electrical energy" at the termination point results in heating, like a soldering iron or element, i.e. a "shorted circuit". The Sea-Urchin *Plasma Core* concept has now been confirmed with "Star in a Jar" developments like the Safire Project, <http://safireproject.com/>, which shows the development of plasma anode tufts in organized energy patterns as the Sea-Urchin model predicts. Repulsive forces in the anode tufts control their energy geometry. While the induction energy mechanism is the key to internal forcing [41, 45].

The induction characteristics are determined by current alignments between layers in the Earth and polarity relationships between of the Earth, Sun and other planets. The alignment and polarity determine the attraction or repulsive forces in *Plasma Core* physics and determine charging and discharging forces on our planet (Fig. 20, 21, 22, and 23). Fig. 21 conceives an idealized *Plasma Core Model of Earth as a Stellar Transformer*.

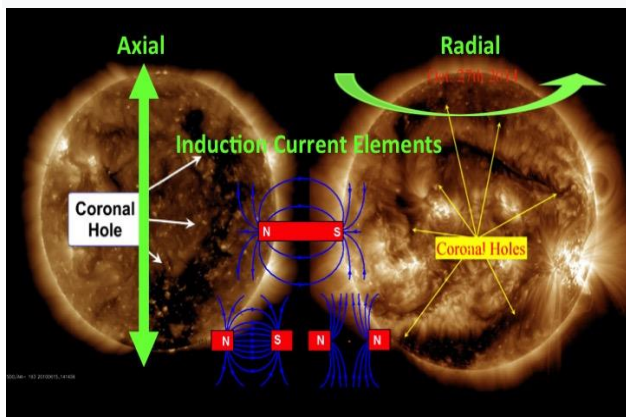


**Fig. 24. Solar Stellar Transformer Coronal Hole Induction Current Elements** express induction elements in axial vs. radial orientations determining axial vs. radial affects on Earth systems. Polarity determines attractive/repulsive force determining charging/discharging relationships [36, 38].

Each vector has a primary effect when considered as separate vectors, but in reality, these are not separable circuits and should be considered together as coupled with the Sun's total variability and output, and ideally with position and magnetic fields of the moon and other planets. To simplify, understanding of the relationships, solar coronal holes that are

aligned with the Sun's north-south polar axis can be considered axial induction elements, while those aligned with the equator can be considered radial induction elements. Many coronal hole configurations represent some combination of the axial and radial elements. This is important to understand because the elements on Earth are directly energized by alignment relationships between these Sun and Earth elements controlled by magnetic moment orbital physics. These dark coronal holes on the Sun represent the induction current elements of our *Solar Stellar Transformer* (Fig. 24), charging/discharging the Sun from elements within the arm of our spiral galaxy and thereby the Solar System including Earth, via electro-magnetic wavelength and frequency response, within an Electric Universe framework [46]. *The alignment and polarity determine the attraction or repulsive forces in plasma physics and determine charging and discharging forces on our planet.*

## 10. CONCLUSIONS

With the inclusion of the orthogonally intersecting megatrends and the fallacies associated with calibrating the magnetic anomalies on the ocean floor, one has to seek umbrage under some other tectonic explanation for the existence of these anomalous findings. The existence of oceanic plateau and rises at many of these intersections leads the astute investigator to examine those features more circumspectly, especially the rock compositions. Many are more granitic. This could be sundered pieces of continents. It could also be the result of some physical force that has as yet been undecided, or even undiscovered. A hypothetical conclusion proposed is that electric transmutation of original crust by global plasma events may produce granite not only mid-ocean, but likely continental elements as well. Thus, ocean basin orthogonal fractures are in-line with, and correspond to, the coils of an *Earth-Sun Stellar Transformer*, where anode tufts or "sea-urchin spikes" emanating from Earth's core intersect the coils. As a result, magnetic moment alignments of Earth's North-South tectonic ridge system with the Sun can influence our daily weather via a noon-midnight induction of lightning on the continents.

The timing and global distribution of Lightning data along with the other environmental relationships exposed in this paper demonstrates a pathway to a new paradigm of understanding solar induction effects on our planet. Geomagnetic effects are inevitable, given the Electro-Magnetic output of the Sun and the fact that earth's core is Magnetic and spinning. These effects may interact with and/or account for many well-known electric phenomena, such as aurora borealis and St. Elmo's Fire. Geomagnetic effects may also affect the weather, through increasing or reducing the frequency and magnitude of Lightning in a local area. This could also lead to potential relationships between geomagnetic effects and Lightning - induced phenomena, such as Wildfires. It is also plausible that the large forces associated with geomagnetic phenomena can impact or trigger phenomena such as earthquakes and volcanoes. The implications to humanity are that Stellar Transformer concepts can be implemented with an improved understanding of common Electro-Magnetic denominators associated with Space Weather hazards such as; Electro-Magnetic Pulse (EMP), communication problems, general every day and extreme weather events, i.e. Hurricanes, Tornadoes associated with the variable frequencies of Climate Change, Earthquakes, Volcanoes, and certain types of wildfire outbreaks associated with Coronal Mass Ejections (CME's).

## 11. REFERENCES

- [1] Meyerhoff, A.A. and H.A. Meyerhoff. **The new global tectonics: major inconsistencies.** *American Association of Petroleum Geologists Bulletin* Vol. 56, No.2, 1972, pp. 269–336.
- [2] Agocs, W.B., A.A. Meyerhoff, and K. Kis, **Reykjanes Ridge: quantitative determination from magnetic anomalies.** In: S. Chatterjee and N. Hotton III (eds) *New Concepts in Global Tectonics* (Texas Tech University Press, Lubbock), 1992, pp. 221-238.
- [3] Smoot, N.C., **Magma floods, microplates, and orthogonal intersections,** *New Concepts in Global Tectonics Newsletter* 5, 1997, pp. 8-13.
- [4] Smoot, N.C., **The Darwin phoenix rises yet again.** *New Concepts in Global Tectonics Newsletter* 14, 2000, pp. 2-4.
- [5] Smoot, N.C., **Ocean Survey Program (OSP) bathymetry history: Jousting with tectonic windmills.** In: J.M. Dickins, A.K. Dubey, D.R. Choi, and Y. Fujita (eds) *Special Volume on New Concepts in Global Tectonics, Himalayan Geology* Vol. 22, No./1, 2001a, pp. 65-80.
- [6] Smoot, N.C. and K.J. Heffner, **Bathymetry and possible tectonic interaction of the Uyeda Ridge with its environment,** *Tectonophysics* 124, 1986, pp. 23-36.
- [7] Smoot, N.C., and A. Lowrie, **Emperor Fracture Zone morphology by multibeam sonar,** *Journal of Geology* 93, 1985, pp. 196-204.
- [8] Lowrie, A., N.C. Smoot, and R. Batiza, **Are oceanic fracture zones locked and strong or weak?: New evidence for volcanic activity and weakness,** *Geology* 14, 1986, pp. 242-245.
- [9] Smoot, N.C., **The Marcus-Wake seamounts and guyots as paleofracture indicators and their relation to the Dutton Ridge,** *Marine Geology* 88, 1989, pp. 117-131.
- [10] Smoot, N.C., **The trans-Pacific Chinook Trough megatrend,** *Geomorphology* Vol. 24, No. 4, 1998a, pp. 333-351.
- [11] Smoot, N.C., **WNW-ESE Pacific lineations,** *New Concepts in Global Tectonics Newsletter* 9, 1998b, pp. 7-11.
- [12] Smoot, N.C. and R.E. King, **The Darwin Rise demise: The western Pacific guyot heights trace the trans-Pacific Mendocino Fracture Zone,** *Geomorphology* Vol. 18, Nos. 3/4, 1997, pp. 223-236.
- [13] Smoot, N.C. and B.A. Leybourne, **The Central Pacific Megatrend.** *International Geology Review* Vol. 43, No. 4, 2001, pp. 341-365.
- [14] Smoot, N.C. and D.R. Choi, **The North Pacific Megatrend,** *International Geology Review* Vol. 45, No. 4, 2003, pp. 346-370.
- [15] Smoot, N.C., *Tectonic Plate Margins* (CreateSpace Independent Publishing Platform, Amazon), 2018, 174 p.
- [16] Leybourne, B.A. and N.C. Smoot, **Ocean basin structural trends based on GEOSAT altimetry data,** in: *Ocean Technology at Stennis Space Center: Proceedings of the Gulf Coast Chapter Marine Technology Society*, 1997, pp. 135-140.
- [17] Smoot, N.C., **Earth geodynamics hypotheses updated.** *Journal of Scientific Exploration* Vol. 15, No. 4, 2001b, pp. 465-494.
- [18] Smoot, N.C., **Fingernails, GPS, and Pacific basin closure.** *New Concepts in Global Tectonics Newsletter* 21, 2001c, pp. 24-25. This one was also reprinted in *The Australian Geologist*, No. 123, June 2002.
- [19] Smoot, N.C., **Seamount chains, fracture zones, and oceanic megatrends,** *Bolletino della Societa Geologica Italiana*, Special Issue: *Earth Dynamics Beyond the Plate Paradigm*, 5, 2005, pp. 25-52.
- [20] Smoot, N.C., **Orthogonal intersections of megatrends in the Mesozoic Pacific Ocean basin: a case study of the Mid-Pacific Mountains,** *Geomorphology* 30, 1999, pp. 323-356.
- [21] Smoot, N.C., **North-central Pacific basin lineaments and mobilism: Really?** *New Concepts in Global Tectonics News-letter* 62, 2012, pp. 5-21.
- [22] Smoot, N.C., **Northern Hess Rise extended by multi-beam sonar,** *Tectonophysics* 89, 1982, pp. T27-T32.
- [23] McKenzie, D. and Sclater, J.G., 1971. **The evolution of the Indian Ocean since the Late Cretaceous,** *Geophysical Journal International* 25:35, 437-528.
- [24] Patriat, P. and Segoufin, J., 1988. **Reconstruction of the central Indian Ocean,** *Tectonophysics* 155, 211-234.
- [25] Dymant, J., 1993. **Evolution of the Indian Ocean triple junction between 65 and 49 Ma.** *Journal of Geophysical Research* 98: B9, 13,863-13,877.
- [26] Masalu, D.C.P., 2002. **Absolute migration and evolution of the Rodrigues triple junction since 75 Ma.** *Tanzanian Journal of Science* 28:2, 97-104.
- [27] Sauter, D., Mendel, V., Rommenaux-Jestin, C., Patriat, P., and Munsch, M., 1997. **Propagation of the Southwest Indian Ridge at the Rodrigues Triple Junction.** *Marine Geophysical Researches* 19:6, 553-567.
- [28] West, B.P., Fujimoti, H., Honsho, C., Tamaki, K., and Sempere, J-C, 1995. **A three-dimensional gravity study of the Rodrigues Triple Junction at the Southwest Indian Ridge.** *Earth and Planetary Science Letters* 133:1, 175-184.
- [29] Masalu, D.C.P., 2015. **Global mid-ocean ridge mantle tomography profiles,** *Earth Sciences* 4:2, 80-88.
- [30] Munsch, M. and Schlich, R., 1989. **The Rodrigues Triple Junction (Indian Ocean): Structure and evolution**

- for the past one million years, *Marine Geophysical Research* 11:1, 1-14.
- [31] Leybourne, B.A. and Adams, M.B., 2001. **El Nino tectonic modulation in the Pacific Basin.** *Marine Technology Society Oceans '01 Conference Proceedings*, Honolulu, Hawaii, Nov. 2001.
- [32] Leybourne, B. A. and Davis, J. M., **Farallon Hyper-Volcano: Mantle Gravity Indicates Circuits: Arc Blast Theoretical and Field Evidence,** *Stellar Transformer Bulletin: Institute for Advanced Studies in Climate Change (IASCC)*, Internal Members Publications: Aurora, CO, USA
- [33] <https://ngdc.noaa.gov/mgg/global/global.html>
- [34] Albrecht, R. I., S. J. Goodman, D. E. Buechler, R. J. Blakeslee, and H. J. Christian, 2016, **Where are the lightning hotspots on Earth?**, *Bulletin American Meteorology Soc.* doi:10.1175/BAMS-D-14-00193.1.
- [35] Christian, Hugh J. , Richard J. Blakeslee, Dennis J. Boccippio, William L. Boeck, Dennis E. Buechler, Kevin T. Driscoll, Steven J. Goodman, John M. Hall, William J. Koshak, Douglas M. Mach, and Michael F. Stewart, **Global frequency and distribution of lightning as observed from space by the Optical Transient Detector,** "J. Geophys. Res., 108(D1), 4005, doi:10.1029/2002JD002347, 2003.
- [36] Leybourne, B.A., J. Davis, G.P. Gregori, J. M. Quinn, and N. Christian Smoot, **Evolution of Earth as a Stellar Transformer,** *New Concepts in Global Tectonics Journal*, V. 5, No. 1, March 2017, pp. 144-155. See: [www.iascc.org/the-science](http://www.iascc.org/the-science).
- [37] Ba, M. B., and S. E. Nicholson, **Analysis of convective activity and its relationship to the rainfall over the Rift Valley Lakes of East Africa during 1983–90 using the Meteosat infrared channel.** *J. Appl. Meteor.*, 37, 1250–1264, doi:10.1175/1520-0450, 1998.
- [38] Leybourne, B.A., **Stellar Transformer Concepts: Solar Induction Driver of Natural Disasters - Forecasting with Geophysical Intelligence,** 2018, *Journal of Systemics, Cybernetics and Informatics*, Orlando, FL, V. 16, N. 4, pp. 26-37, ISSN: 1690-4524. <http://www.iiisci.org/journal/sci/FullText.asp?var=&id=IP053LL18>
- [39] Knudsen, Per, Ole Andersen, Shfaqat Abbas Khan, and Jacob Høyer, **Ocean tide effects on GRACE gravimetry,** 8 p. in *Sideris (2001)*. Sideris, Michel G., (ed.), 2001. Gravity, geoid, and geodynamics 2000, *IAG Symposia*, 123, 398 pp., Springer-Verlag, New York.
- [40] Vine, F. J., & Matthews, D. H. (1963). Magnetic Anomalies Over Oceanic Ridges. *Nature*, 199(4897), 947-949.
- [41] Gregori, G.P., **Galaxy-Sun-Earth Relations: The origins of the magnetic field and of the endogenous energy of the Earth,** *Arbeitskreis Geschichte Geophysik*, ISSN: 1615-2824, Science Edition, W. Schroder, Germany, 2002.
- [42] Tukey, John W., *Exploratory data analysis.* Addison-Wesley Publ. Co., Reading, Mass. – Menlo Park, Cal., London, Amsterdam, Don Mills, Ontario, Sidney, XVI, 688 pp., 1977.
- [43] Smoot, N.C. and B.A. Leybourne, 2020, **Orthogonal Megatrend Intersections: “Coils” of a Stellar Transformer,** *Proceeding 11<sup>th</sup> International Multi-Conference on Complexity, Informatics, and Cybernetics*, Orlando, pp. 61-66, Orlando, FL, March 2020  
Also See: *Journal of Systemics, Cybernetics and Informatics*, Orlando, pp. 62-69, V. 18:N. 2, Orlando, FL, March 2020. ISSN: 1690-4524 (Online)  
<http://www.iiisci.org/journal/sci/FullText.asp?var=&id=ZA964ZZ20>
- [44] Hawthorne Jr., R., 2020, **Electric Discharge - Not an Impact Caused Formation Of Upheaval Dome, Canyonlands National Park, Utah,** *Conference Proceeding, Journal of Systemics, Cybernetics and Informatics*, Orlando, FL, March 2020 (Pending Publication).
- [45] Gregori, G.P., 2014. **Climate and the atmospheric electrical circuit: the electromagnetic coupling between solar wind and Earth.** *NCGT Journal*, v. 2, no. 1, p. 99-112.
- [46] Thornhill, W. and Talbott, D., 2007. *The Electric Universe*, Mikamar Publishing (May 24, 2007), 132p.